Investigation of Coefficient of Friction at The Interface of Automobile Brake Pads Using Greenwood-Williamson Contact Model and Novel Test Rig

Mrunal P. Kshirsagar
Research Scholar
Veermata Jijabai Technological Institute
Department of Mechanical Engineering
India

Hrishikesh Khairnar
Assistant Professor
Veermata Jijabai Technological Institute
Department of Mechanical Engineering
India

Different brake pad materials are produced, each with their unique composition in the recent past, yet performing the same task and claiming to be better than others. The article provides references for different automotive brake pads subjected to various operating conditions. The present investigation develops an analytical approach for estimating COF and contact radius for different disc-brake pads, which can be used to design an efficient automotive brake pad-disc system under the given load and rotational speed. The coefficient of friction at the pad-disc interface is investigated considering Greenwood Williamson (GW) model and developed novel friction test rig. A MATLAB program along with FFT was developed to simulate the surface topography of the contact interface during the braking process aiding the estimation of contact radius. Surface topography of tested brake pads has been analyzed using an infinite-focus-microscope to verify contact radius. At last, the reference is verified by an experimental investigation using a developed test rig and considering operating parameters.

Keywords: *Brakes, Coefficient of friction, contact mechanics, interfacing surface, Tribology.*

1. INTRODUCTION

Automotive brakes play a vital role in the active safety of the vehicle. Today almost all vehicles use a disc brake system, which consists of a minimum of two pads and a disc for a signal wheel. Various friction materials for the brake pad are constantly manufactured and tested to improve braking efficiency. With the increasing demand for accuracy, the contact interface between brake pad and disc is studied for the interest in contact and frictional phenomena to make it as precise as possible.

A considerable part of research in this field is concentrated on finding methods for implementing simple contact conditions and Coulomb's law of friction. At the forefront is the search for the most efficient algorithms possible regarding calculation time and implementation costs. Contact is typically seen as a one-sided rigid constraint. For the laws of friction, it is assumed that a maximum force of static friction exists and that the force of kinetic friction depends on sliding velocity. Frequently, the force of kinetic friction is considered constant and equal to the maximum force of static friction. The frictional force is independent of the nominal or apparent area of the surfaces in sliding contact. [1]

The theory regarding the interaction of friction and wear in the interface shows that the tribological beha–vior of the system, which is determined by the growth and destruction of characteristic hard structures ('patches') on a mesoscopic length scale, was studied by G.P. Ostermeyer et al. [3]. H. P. Khairnar et al., [4] investigated encompasses a multitude of equations for friction coefficient derived under the equilibrium condition using principles of classical mechanics with friction considering the variations of longitudinal forces. The correlation of temperature, contact pressure, friction force and friction coefficient were described. Although extensive research work has been carried out in the field of automotive braking systems regarding the depen–dency of the friction coefficient (μ) at the brake disc-pad interface on various parameters like velocity, contact pressure, temperature, and different compositions of materials [4-7]. Yet there is not much work carried out in analyzing the effects of the actual contact force, actuating force, and Coulomb friction force on the friction coefficient (μ).

The brake disc speed is high at working, which forms the debris by shearing action of the friction material and some particles expelled out of the contact interface. The friction surface film layer influences the brake system's friction and wears behavior [3,9,10]. The friction film layer is made of primary plateaus of hard particles and fibers and secondary plateaus of piling up wear debris and compacted against the primary plateaus [11-13]. Friction, wear, and emission performance were strongly affected by creating secondary plateaus of the cermet-coated disc. During braking, the topography of the disc surface changes, resulting in changes in the pad-to-disc contact situation regarding pressure and contact area [14,15]. In the braking process, friction heat is always generated between brake friction pairs,

Received: April 2022, Accepted: August 2022
Correspondence to: Mrunal P. Kshirsagar, Veermata Jijabai Technological Institute, Department of Mechanical Engineering, Mumbai, India-400019
E-mail: mrunalkshirsagar19@gmail.com
doi:10.5937/fme2203561K

which has a significant impact on the mechanical and physical properties of the friction material surface [16]. Particularly, under intense braking conditions of high speed and overload, the friction surface temperature will rise rapidly to an extremely high value, and then disastrous friction anomalies will easily arise [20-21].

Dynamic change in the size and composition of the contact area has a crucial influence on the friction behavior of the disc brake and, accordingly, braking phenomena generation[21].

The contact situation between a cast-iron brake disc and friction materials primarily influences the perfor–mance of the brake [31]. To numerically simulate the behavior of brakes is realistic, it is essential to accu–rately represent the frictional behavior at the contact interface. The complexity of the interactions between the different parameters determines the difficulty of reliable and exact frictional laws [8]. Unfortunately, many researchers use classic laws of friction in their sophisticated finite element analysis, which is insu–fficient. As discussed in detail in [17], the conventional analytical approaches cannot handle modeling errors and suffer from lack of accuracy and robustness. Similarly, C. Hohmann [30] has used the sparse solver implemented in ADINA Version 7.1 to reduce job duration time for contact analysis. But again, practically if we consider the OMEs that design the brake system for various applications will not always invest in such high-end software. The correct calculation of contact is essential for the design of friction brakes.

Velocity, loading, braking moment, temperature, and wear are linked and depend on friction pair friction, mechanical and thermos-physical properties, as well as design and regime of exploitation[22]. In a short time, repeating braking regimes is arduous by considering impact factors: load, pressure, and velocity. The present work develops a mathematical model using classic contact mechanics laws. This research aims to develop and test the mathematical model to predict the coefficient of friction by considering the material surface properties of the brake pad and disc. The contact mechanics between the interfaces of braking parts are studied to establish a causal relationship between the different parameters that leads to a reduction in performance or complete failure of the braking system. The model was further tested on the brake friction test set-up. A MATLAB program is developed to stimulate the brake pad surface during contact. Its further testimonies are provided by surface analysis using an infinite focus microscope on the tested brake pad samples. The research results allow prognosticating the actual coefficient of friction linings already in the design stage and allow for choosing the most suitable friction lining material for manufactural needs.

2. FRICTION AND CONTACT MECHANICS

Sliding friction between two dry contacting surfaces is often known as 'Coulomb friction' after Charles Cou–lomb (1736-1806) [23]. Still, despite its everyday nature, the friction forces involved can usually only be estimated from previous experience and experimental evidence. 'Transfer films' are often used to coat the surfaces in friction brakes due to the sliding process so that the surfaces in contact are not just bare metal or friction material. A friction surface is rough on the microscopic scale, although it appears geometrically smooth and has a distribution of asperities. One explanation of the genesis of friction is the interaction of microscopic asperities on the two surfaces. Model systems have been studied in which the materials and surfaces were scientifically controlled in the expectation that once the friction of such systems was understood, more and more complicated systems could be examined [23].

The frictional force is independent of the nominal or apparent area of the surfaces in sliding contact. A simple physical explanation of the frictional laws relates to the difference between the 'real' area of contact Ar (based on the total surface areas of the microscopic asperities in contact) and the 'apparent' (or 'nominal') area of contact An (indicated by the overall size of the contact interface) at any friction interface or a complete understanding of the phenomenon of friction it would be necessary at the very least to be able to determine Ar. Still, the more this is investigated, the more complicated it appears. There is no easy way to do this for the friction material pairs used in modern automotive braking systems [5]. Thus, using the theories for contact mechanics ensures to development of an analytical model for the estimation of COF between the disc-pad brake interface.

The early investigation in this field was made by Greenwood and Williamson [2]. They discovered that many important properties of the contact are almost independent of the local asperity behavior of the asperity height distribution in Gaussian. When the distribution of the identical asperities is exponential, they found linear relations between the total load, thermal and electrical contact conductance, and the whole contact area, regardless of the constitutive law describing the contact process of the actual contact area. In the G-W framework [28], the contact between two rough surfaces is modeled as a contact problem between a rigid flat surface and an elastic solid decorated with a randomly rough surface, which is further assumed to be an ensemble of non-interacting spherical asperities of the same curvature radius R (see Fig.1 for reference). It is extensively used to calculate microcontact and pressures that arise when two rough surfaces approach each other. One surface is considered to have the combined roughness of the two original surfaces, and the other is considered smooth.

It is worth noting that the idea underlying the G-W's approach has also been generalized to establish models of a rough surface with multiple representative shapes and curvature radii [29].

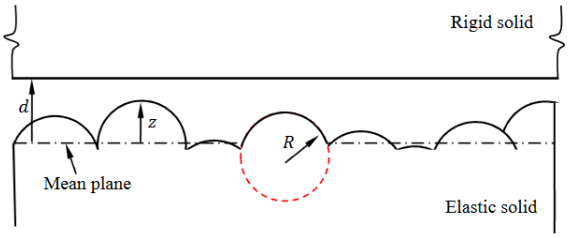

Figure 1. Greenwood Williamson model for rough contact.

To conclude, the GW model is a basic model for calculating pressure between two flat surfaces consi–dering their physical material properties. The proposed mathematical model applies the GW model on the brake pad-disc surface to calculate the pressure accurately.

3. ANALYTICAL INVESTIGATION:

During braking in automobiles, there is a dynamic transfer of (70%) of total weight onto the front wheels of a vehicle with a corresponding decrease at the rear wheels (30%) [2], as shown in fig 2. Fig 3 illustrates the forces acting on the wheels of the vehicle while braking, where F_f is the frictional force acting on the front wheel and Fr is the frictional force acting on the rear wheel.

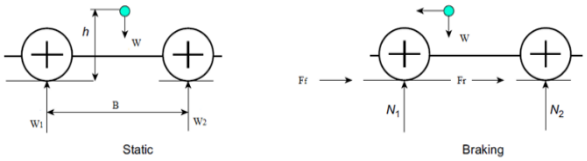

Figure 2. Dynamic effect on the vehicle during the static and braking conditions

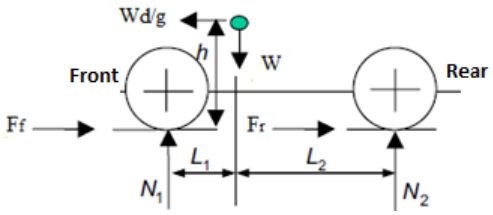

Figure 3. Forces during braking.

N_1 and N_2 are the normal forces acting on the front and rear wheels, respectively.

The moments on rear wheels with the road give:

$$N_1\left(L_1+L_2\right)-WL_2-W\frac{d}{g}h=0 \tag{1}$$

At rest, as the deceleration (m/s^2) is d=0, the weight of the vehicle is transferred to the front wheels, thus,

$$d=0;\ W_1=\frac{WL_2}{L_1+L_2} \tag{2}$$

Therefore, the normal reaction force on the front wheel is calculated as follows and is given by (3),

$$N_1=F_f\left[\frac{L_2}{L_1+L_2}+\frac{d/g}{L_1+L_2}\right]=W_1+\frac{W\left(d/g\right)h}{B} \tag{3}$$

Similarly, at the rear wheels, the normal force can be given accordingly by rearranging the terms in mass moments and forces.

$$N_2=F_r\left[\frac{L1}{L_1+L_2}+\frac{d/g}{L_1+L_2}\right]=W_2-\frac{W\left(d/g\right)h}{B} \tag{4}$$

Forces N_1 and N_2 are opposed by the clamping force produced in the brake system, which acts in the opposite direction and aid in stopping or deaccelerating the vehicle.

The front and rear brake forces are the product of applied pressure on the brake times per axel by tire radius, which is given in the following equation, where G_f and G_r are brake gain for front and rear axle, respectively P_f and P_r are pressure applied by brake cylinder. [25]

$$F_f=2G_f\frac{P_f}{r};\ F_r=2G_r\frac{P_r}{r} \tag{5}$$

Deceleration is the sum of brake forces divided by total vehicle weight, as given in (6)

$$D_x=\frac{F_{xf}+F_{xr}}{w} \tag{6}$$

Accordingly, the front and rear axle loads are calculated as follows, considering the moment forces acting on the axle and the vehicle's deceleration during braking action.

$$W_f=W_{fs}+\left(\frac{h}{L}\right)\left(\frac{w}{g}\right)D_x \tag{7}$$

$$W_r=W_{rs}-\left(\frac{h}{L}\right)\left(\frac{w}{g}\right)D_x \tag{8}$$

Now, the brake force produced between the brake pad and disc interface can be represented by,

$$F_f=P\times A \tag{9}$$

The clamping force, which acts on the back plate of the brake pad, is calculated as follows by considering the force applied by the driver (F_d), M_l- mechanical leverage, and H_l- hydraulic leverage.

$$F_c=F_d\times M_1\times H_1\times 2 \tag{10}$$

The braking torque is calculated by undertaking the dynamic axel weight (W_t) and the diameter of the tire (D_w)

$$T_b=\frac{W_t}{2}\times\frac{D_w}{2}\times g \tag{11}$$

Accordingly, the tangential force (F_t) has been calculated as given in the following (12) by considering the raking torque as calculated in (11) and active radius (r_a) where the force is applied on the brake disc through the brake pad.

Tangential force,

$$F_t=\frac{T_b\left(Braking\,Torque\right)}{r_a} \tag{12}$$

The force applied on the disc during braking is given by the following (13),

$$F_x=\frac{F_c\left(total\,clamping\,force\right)}{2} \tag{13}$$

And resulting frictional force is given by (14.1), where μ is the coefficient of friction between the brake disc and brake pad.

$$F_t=F_x\times\mu \tag{14}$$

$$\mu=\frac{F_t}{F_x} \tag{14.1}$$

Equation (14.1) has been used for calculating the COF of a brake system by using (13) for F_x in which clamping force is calculated through (14) and F_t is calculated by using (14).

This damping force is generated hydraulic which can be calculated as,

$$F = P_a \times a \tag{14.2}$$

where P_a is pressure to the hydraulic cylinder and a is an area of bore,

$$F_C = P_a \times \frac{\pi d^2}{4} \tag{14.3}$$

Also, torque at the rotor will produce tangential force opposing the clamping force.

The clamping force is divided into two discs on the back plate. This force is given to each disc,

$$F_d = \frac{1}{2}\left(\frac{P_a \times \pi \times d^2}{4}\right) \tag{15}$$

$$P_a = \frac{8F_d}{\pi d^2} \tag{16}$$

This pressure is distributed over the area of the disc pad. It was considering a rough surface of the pad, which has a surface roughness R_a.

So, according to the Greenwood Willson (GW) model contact mechanics, the asperities on the disc pad are Gaussian distributed [25], and the pressure of each of the asperities is given by P given as,

$$p = \frac{3W}{2\pi a_i^2} \tag{16.1}$$

where, a = contact radius and w = load

Now, we can assume that,

$$P_a = \sum_{i=1}^{z} \frac{3W}{2\pi a_i^2} \tag{16.2}$$

z = number of asperities

Now, determine the contact radius between the brake and pad interface.

According to contact mechanics theory, applying the theory of contact mechanics inform of GW model to the contacting interface,

$$a = \sqrt[3]{\frac{3WR^*}{4E^*}} \tag{16.3}$$

where,

$$\frac{1}{E^*} = \frac{1-v_1^2}{E_1} + \frac{1-v_2^2}{E_2} \tag{16.3.1}$$

$$z(x) = \frac{1}{\sqrt{2\pi\sigma^2}} \times e^{-\frac{(x-a)^2}{2\sigma^2}} \tag{16.3.2}$$

But for the rotor, it is considered as a flat and smooth surface without any deviation as compared to the disc pad, therefore,

$$\frac{1}{R_2} = 0 \tag{16.3.3}$$

Hence, (16.3.2) becomes,

$$\frac{1}{R^*} = \frac{1}{R_1} \tag{16.3.4}$$

Now, the radius of curvature of disc pad considering Greenwood and Williamson model (GW) model, assuming the height of the asperities are normally, or Gaussian distribution and R is given by,

$$R_1 = \frac{\sqrt{1+z'\left(x^3\right)}}{\left|z''("x)\right|} \tag{16.4}$$

where z(x) is the function of the height of asperities.

Interfacial roughness plays a key role in the mecha–nical behavior of contacting bodies with significant implications for force transfer, friction, wear, and adhesion processes. [26]. The surface roughness, consi–dered an important issue, should be considered. The contact pressure's magnitude and distribution are very sensitive to surface roughness [32]. Roughness or surface roughness R_a is the arithmetic mean of deviated of all the mean values in the assumed profile for the aspirated profile.

$$P = \frac{2}{\pi}\frac{E^*}{R^*}\left[2\sigma^4 \ln\left(R_a \cdot l \cdot 2\pi \cdot \sigma^4\right) + l\right] \tag{17}$$

where, $z(x) = \frac{1}{\sqrt{2\pi\sigma^2}} \times e^{-\frac{(x-a)^2}{2\sigma^2}}$

$$R_a = \frac{1}{l}\int_0^l \frac{1}{\sqrt{2\pi\sigma^2}} \times e^{-\frac{(x-a)^2}{2\sigma^2}}\, dx \tag{17.1}$$

Solving (17.1),

$$R_a = \frac{1}{l}\left[\frac{1}{\sqrt{2\pi\sigma^2}}\left(-e^{-\frac{(x-a)}{2\sigma^2}} \times \frac{-1}{2\sigma^2}\right) + c\right]_0^l \tag{17.1.1}$$

z (0) =0 hence,

$$R_a = \frac{1}{l}\frac{1}{\sqrt{2\pi\sigma^2}}\left(-e^{-\frac{(x-a)}{2\sigma^2}} \times \frac{-1}{2\sigma^2}\right) + c \tag{17.1.2}$$

c<<<1

therefore, (17.1.2) becomes,

$$R_a = \frac{1}{l}\frac{1}{\sqrt{2\pi\sigma^2}}\left(-e^{-\frac{(x-a)}{2\sigma^2}} \times \frac{-1}{2\sigma^2}\right) \tag{17.1.3}$$

Rearranging the terms in (17.1.3),

$$R_a \cdot l \cdot 2\pi \cdot \sigma^4 = e^{-\frac{(l-a)}{2\sigma^2}} \tag{17.1.4}$$

Taking logs from both sides,

$$\ln\left(R_a \cdot l \cdot 2\pi \cdot \sigma^4\right) = -\frac{(l-a)}{2\sigma^2}\ln(e) \tag{17.1.5}$$

$$a = 2\sigma^4 \ln\left(R_a \cdot l \cdot 2\pi \cdot \sigma^4\right) + 1 \qquad (17.2)$$

a is contact radius which varies according to length (l), roughness (R_a), and σ(density of surface).

Thus, determining contact radius real area of contact can be determined.

The pressure can hence determine as follows,

$$P = \frac{2}{\pi}\frac{E^*}{R^*}\left[2\sigma^4 \ln\left(R_a \cdot l \cdot 2\pi \cdot \sigma^4\right) + l\right] \qquad (18)$$

MATLAB model for generating surface brake pad surface.

3.1 ESTIMATION OF REAL CONTACT RADIUS

As mentioned in (16.2), contact radius constitutes many variables, which are properties of materials. For simp–lify the calculations, a MATLAB program was used to generate a random Gaussian rough surface, as shown in fig 5, by considering the following values as input. The flow chart of the MATLAB program is shown in fig 4.

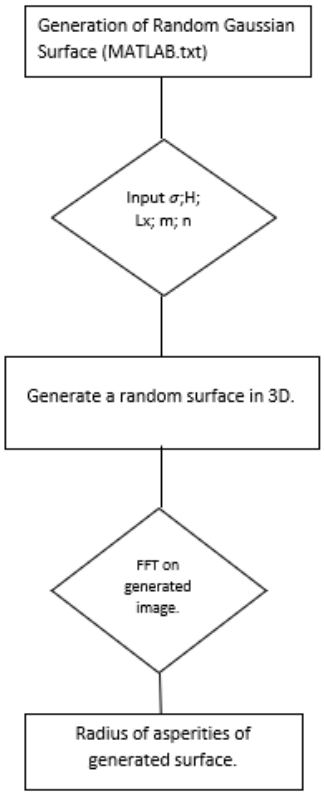

Figure 4. Flow Chart of MATLAB Program

Input parameters:
σ: Standard deviation, i.e., root-mean-square roughness Rq(m) = 13.9
H: Hurst exponent (roughness exponent), 0<= H <= 1= 0.8
Lx: length of topography in x direction. = 10 cm
m: number of pixels in x= 512
n: number of pixels in y= 512

The height of asperities was then obtained by applying a power spectrum technique to the above topography, which is between 12-15 µm. Considering material values of E and υ [24], E* was calculated. E*= 0.347; R*=0.15µm; δ*=13.92.

By inputting the above values in equations (16.2), (12), (14.3), and (14.1), further computations are done.

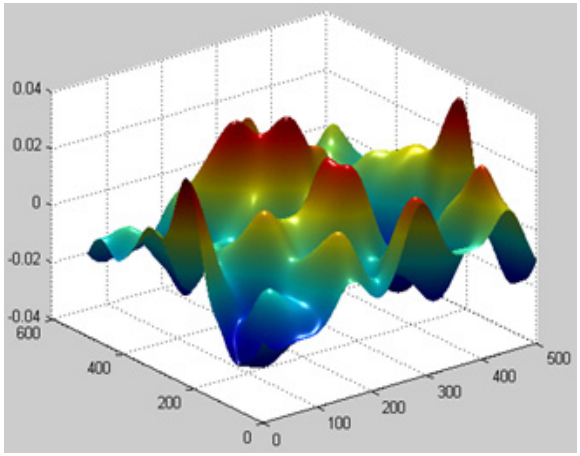

Figure 5. Random Gaussian Surface.

The contact radius of the asperities was calculated by applying Fast Fourier Transform (FFT) on the obtained image in MATLAB, and the radius of asperities was obtained. This radius of asperities is further used for calculating the COF.

The algorithm shown in fig 6 is used for the estimation of COF.

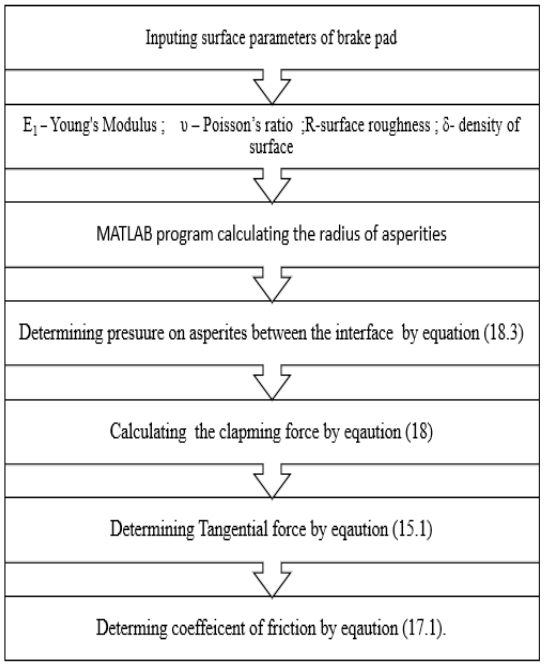

Figure 6. Algorithm for Estimation of COF

4. EXPERIMENTAL INVESTIGATION

An experimental set-up of disc brake testing has been designed for finding brake torque, brake fluid pressure, and coefficient of friction. Test rig comprises motor, brake torque assembly, and disc brake assembly, which are mounted on a suitable and sturdy frame as shown in the schematic diagram in fig 7. Fig 8 and 9 are of the friction brake pad and brake disc used in the set-up. For each rpm the brake pad was changed for obtaining the surface profile at each varying rpm, and easy to analyze. In total, five different sets of brake pad were used.

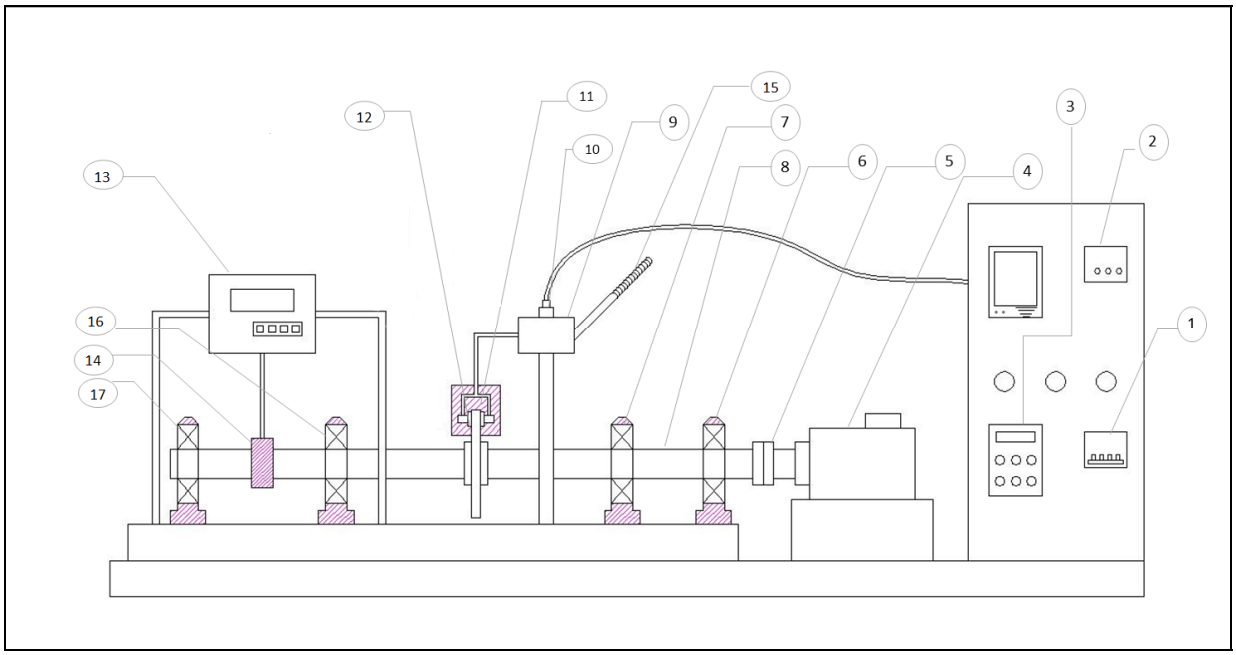

Figure 7. Schematic Diagram of Disc brake set-up.

where, (1) Power Supply, (2) Pressure Display, (3) Variable Frequency Drive (VFD), (4) AC motor-3.7 kW, (5) Coupling, (6) (7) (16) (17) Bearings, (8) Main Shaft, (9) Hydraulic Oil Reservoir (10) Pressure Sensor, (11) Brake Calliper, (12) Brake pads and Disc Mounting Unit, (13) Load Cell, (14) Loading Arrangement, (15) Lever.

Figure 8. Friction brake pad (Brake Linear)

The design of the experiment has been done accor–ding to the capacity of the test mentioned above set-up in fig. 10. As the range of speed for the motor is 0- 1000 rpm, the trials were conducted between the mentioned range. The load applied for the brake is between 0-10 kg. Thus, during experimentation, the load is considered accordingly. By using the DOE, the testing procedure has been planned. A sliding distance of 1000 mm, i.e., 1km is considered with an arm length of 0.22m. Accordingly, various rpm time is set for each cycle.

Figure 9. Brake Disc (Rotor Disc)

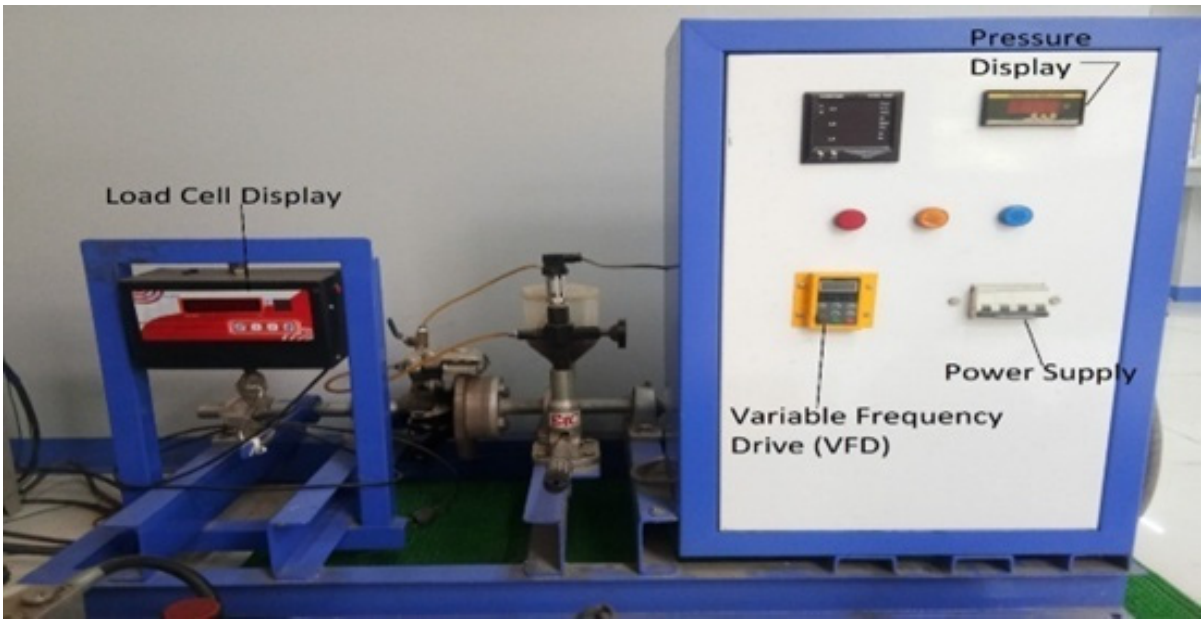

Figure 10. Novel Test Set-up

Table 1. Experimental data of Test rig

RPM	Load (N)	Torque (Nm.)	Pressure(N/mm2)	Force(N)	COF	TEMP
200	20	4.4	0.14	175.84	0.243	66.7
	40	8.8	0.17	219.80	0.389	78.2
	60	13.2	0.2	251.20	0.510	84.2
	80	17.6	0.25	314.00	0.544	97.8
400	20	4.4	0.14	182.12	0.235	93.2
	40	8.8	0.18	229.85	0.372	117.8
	60	13.2	0.21	261.25	0.491	136.9
	80	17.6	0.23	290.14	0.589	177.3
600	20	4.4	0.15	187.14	0.228	93.5
	40	8.8	0.18	233.62	0.366	122.7
	60	13.2	0.21	263.76	0.486	147.4
	80	17.6	0.23	290.14	0.589	202.1
800	20	4.4	0.15	189.66	0.225	112.9
	40	8.8	0.19	238.64	0.358	158.4
	60	13.2	0.22	278.83	0.460	179.3
	80	17.6	0.25	315.26	0.542	234.7
1000	20	4.4	0.14	172.07	0.248	127.1
	40	8.8	0.14	182.12	0.469	184.2
	60	13.2	0.16	202.22	0.634	230.6
	80	17.6	0.21	266.27	0.642	289.2

Experimentation on the test rig was conducted at various rpm, and each time disc pad was replaced. Thus, it gives five samples for separate rpm. This five-disc pad was further processed by gently cutting it out through the base pad and then tested under an Alicona microscope to determine the surface properties of the experimented brake pads.

5. RESULTS AND DISCUSSION:

Alicona microscope provided surface data and images of the brake pad surface in 2D and 3D form. Following fig 11 represents the surface profiles for the various rpm. For each sample, two images were generated, 2D and 3D, respectively, depicting the surface profile of the brake pad material. Also, data such as surface roughness. Below, fig 11 (a) and (a') show the 2D and 3D profiles of the brake pad after 200 rpm, respectively. The average roughness value of 902.35 nm was recorded for the same. Maximum height of Rmax =6.154 μm is noted, with can be seen in fig 10 b with yellow color, and depressions on the surface can be seen in violet. The 2D images show surface profiles of the brake pad surface after braking operation. It depicts the undulation of asperities on the brake pad surface, which come in contact with the iron of the brake disc during braking operation. Similarly values of the rest of table no 2.

Table 2. Profile data for various RPM

RPM	200	400	600	800	1000
Name	Value	Value	Value	Value	Value
Ra	902.36 (nm)	1.395 (μm)	432.01 (nm)	518.54 (nm)	693.71 (nm)
Rq (μm)	1.136	1.851	522.26	686.45	923.69
Rt (μm)	7.117	12.258	2.835	4.134	5.347
Rz (μm)	4.574	7.056	1.970	3.069	4.242
Rmax (μm)	6.154	12.26	2.427	4.054	5.347
Rp (μm)	4.471	8.238	1.364	1.679	2.395
Rv (μm)	2.646	4.020	1.471	2.455	2.952
Rc (μm)	3.603	5.911	1.543	2.433	3.086
Rsm (μm)	210.87	197.5	144.24	236.74	185.24
Rsk	0.538	0.738	0.024	-0.334	-0.352
Rku	3.826	5.115	2.529	3.881	3.498
Rdq	0.064	0.085	0.032	0.039	0.060
Rt/Rz	1.556	1.737	1.439	1.347	1.261
l (mm)	2.814	2.814	2.814	2.814	2.777
Lc (μm)	250	250	250	250	250

Ra - Average roughness of profile;
Rq - Root-Mean-Squareroughness of the profile;
Rt - Maximum peak to valley height of roughness profile; Rz-Mean peak to valley height of roughness profile ; Rmax - Maximum peak to valley height of roughness profile within a sampling length ;
Rp - Maximum peak height of roughness profile ; Rv - Maximum valley height of roughness profile ;
Rc - Mean height of profile irregularities of the roughness profile
Rsm - Mean spacing of profile irregularities of roughness profile.
Rsk - Skewness of roughness profile;
Rku - Kurtosis of roughness profile;
Rdq - Root-Mean-Square slope of roughness profile;
Rt/Rz - Extreme Scratch/Peak value of roughness profile, (>=1), higher values represent larger scratches/peaks;
l - Profile Length;
Lc - Lambda C: cut-off wavelength

It can be clearly stated with images shown in fig 11, that there are patches of material due to wear, thus confirming the formation of plateaus. The Rt/Rz value, i.e., extreme scratch/peak value of roughness profile (>=1), represents the same. In Fig 11 (e'), there is not much deviation seen as the color of the surface is in red shades. This is due to high speed, i.e., at 1000 Rpm, wear rate is higher, and welding of wear particles to surface is caused by high interface temperature. The data obtained by the Alicona microscope is very useful for understanding the topography of the brake pad during various rpm. Also, measurement of each asperity was recorded, which helps in determining the radius of curvature of the asperity. This radius of curvature is geared towards calculating the area of contact between the interfacing surface during the braking process. By using (19.2), i.e.

$$a = 2\sigma^4 \ln\left(Ra \cdot l \cdot 2\pi\sigma^4\right) + l$$

the radius of contact is determined by inputting the data from table no 2, which is used for further calculation of COF. The calculated value of the radius of asperity, force, and COF are tabulated in table no 3.

The COF of the braking system is determined by equation (17.1) which is usually used in the industry; hence, here, it is mentioned as nominal COF and the COF det–ermined by using the algorithm as given in Fig 6 is mentioned as derived from equation COF. Accor–dingly, the results of both methods are presented and further discussed.

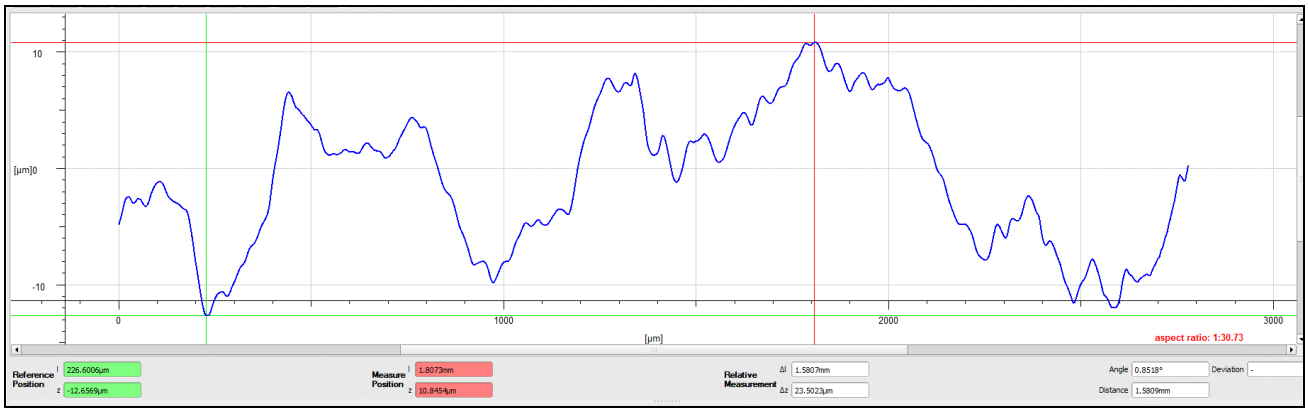

(a)

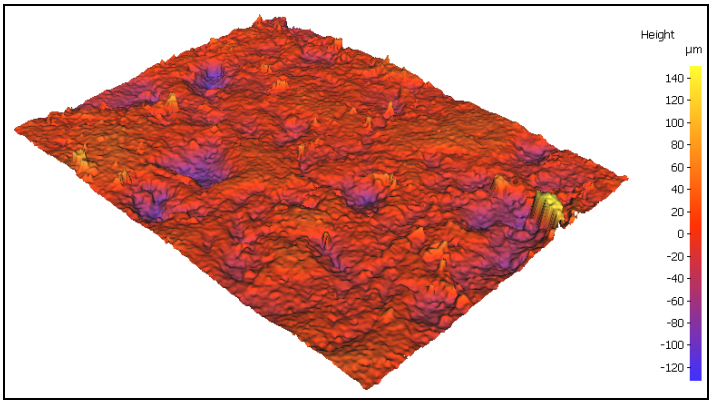

(a')

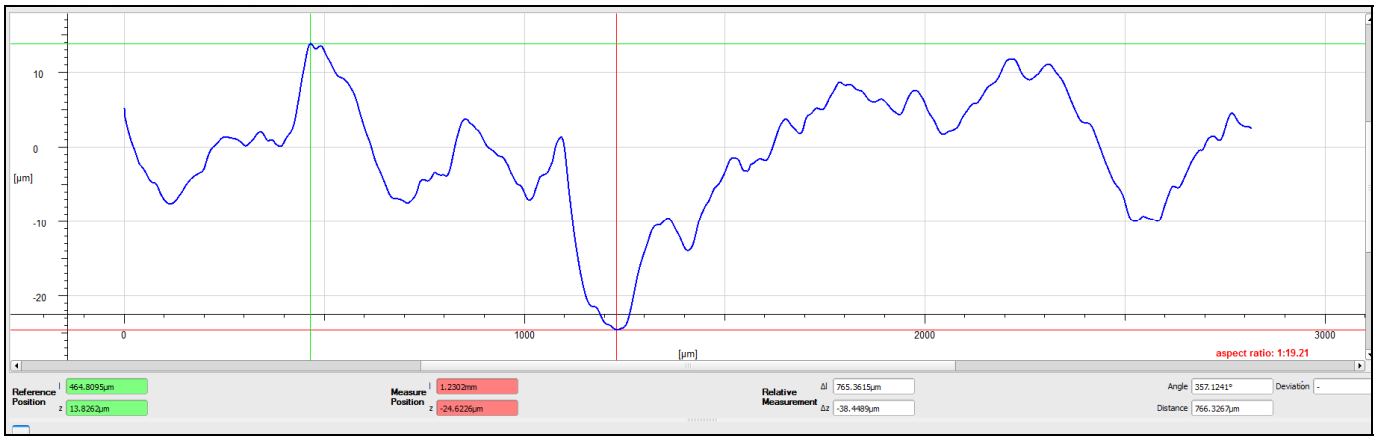

(b)

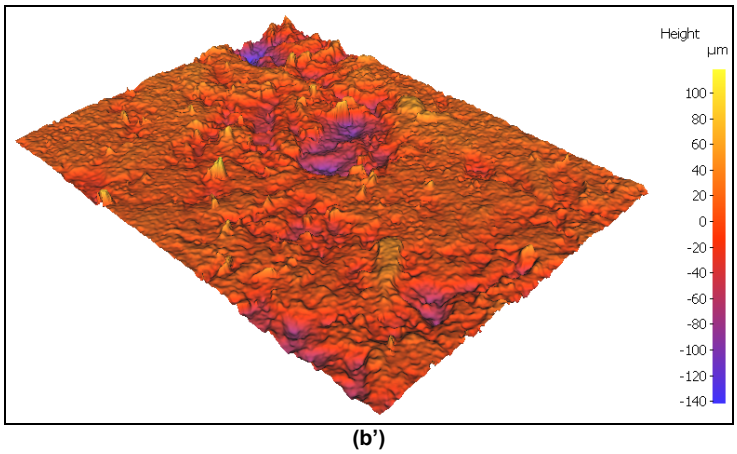

(b')

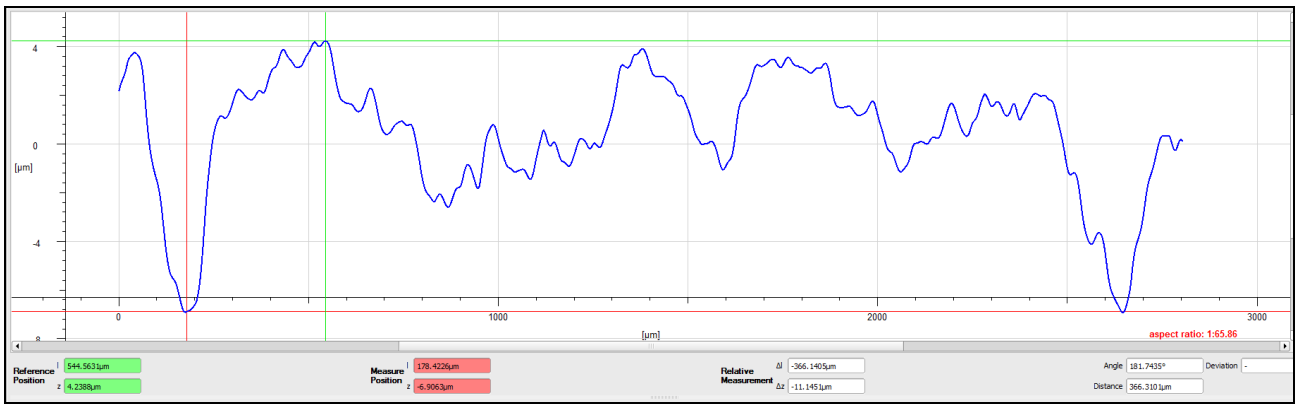
4
0
-4
[µm]
0
1000
2000
3000
[µm]
aspect ratio: 1:65.86
Reference Position
544.5631µm
4.2388µm
Measure Position
178.4226µm
-6.9063µm
Relative Measurement
Δl -366.1405µm
Δz -11.1451µm
Angle 181.7435°
Deviation -
Distance 366.310µm

(c)

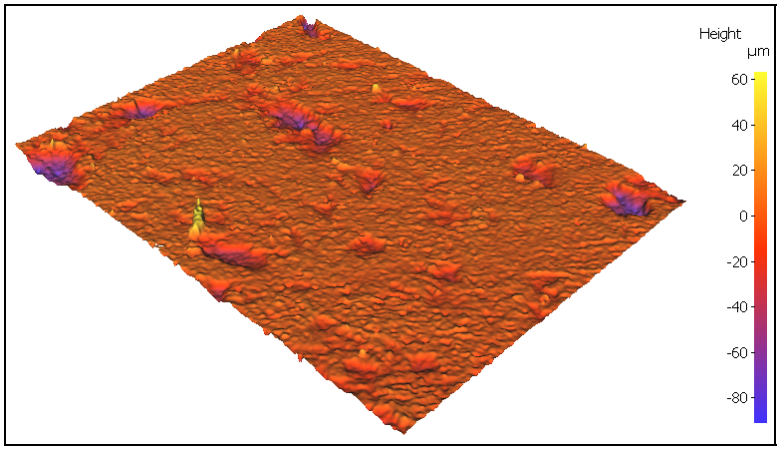
Height
µm
60
40
20
0
-20
-40
-60
-80

(c')

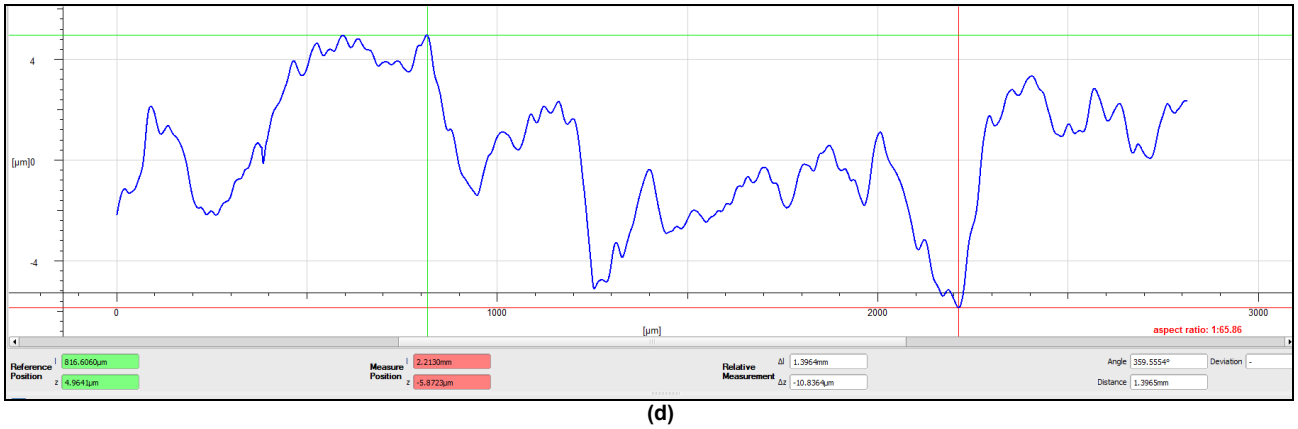
4
[µm]0
-4
0
1000
2000
3000
[µm]
aspect ratio: 1:65.86
Reference Position
816.6060µm
4.9641µm
Measure Position
2.2130mm
-5.8723µm
Relative Measurement
Δl 1.3964mm
Δz -10.8364µm
Angle 359.5554°
Deviation -
Distance 1.3965mm

(d)

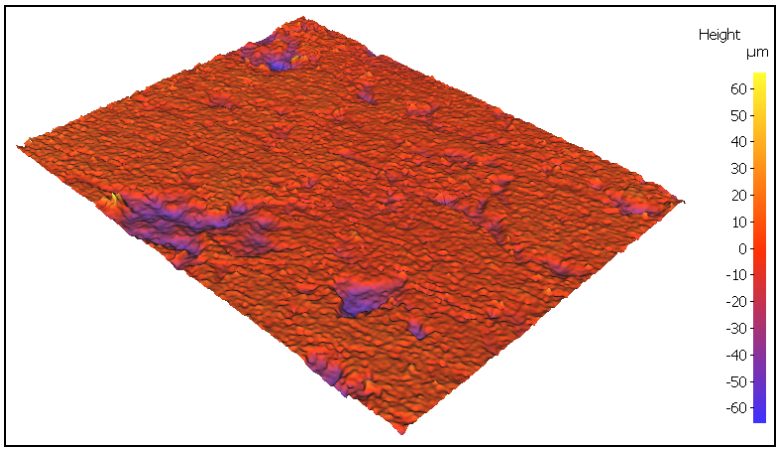
Height
µm
60
50
40
30
20
10
0
-10
-20
-30
-40
-50
-60

(d')

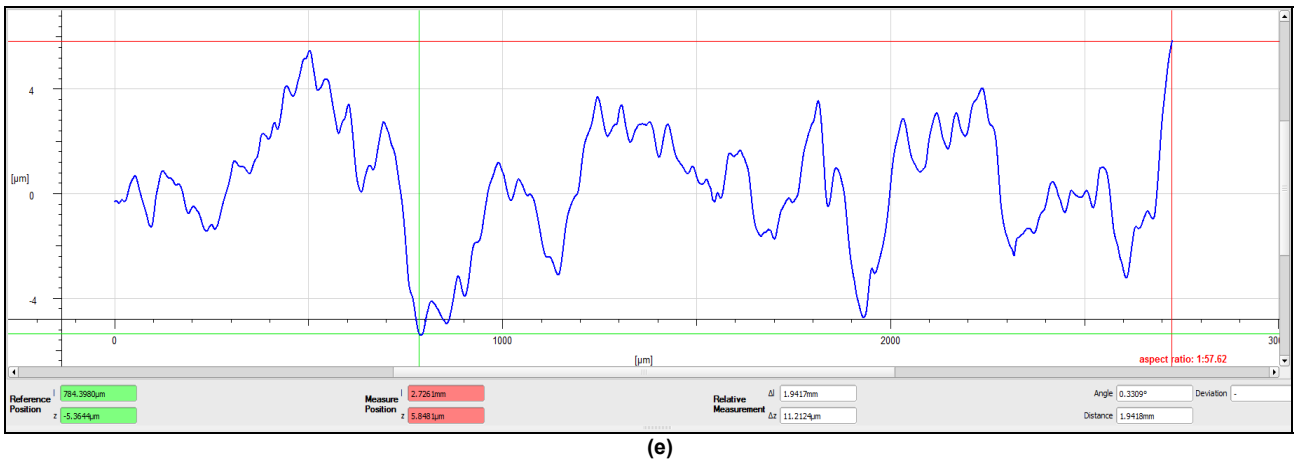

(e)

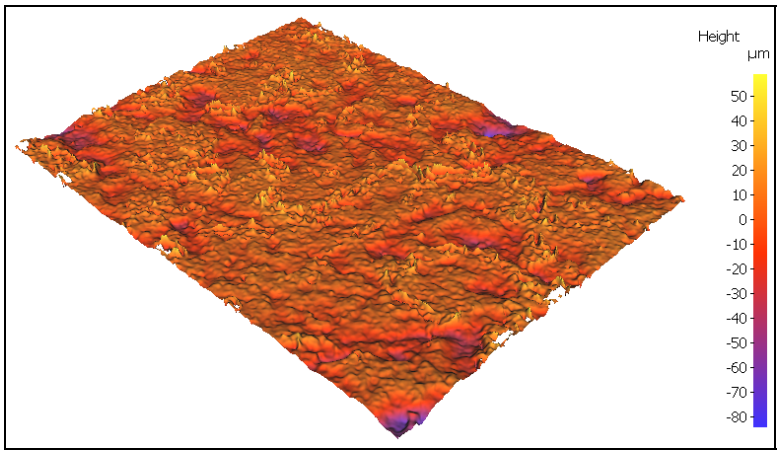

(e')

Figure 11. 2D Profile image for (a) 200 Rpm, (b) 400 Rpm, (c) 600 Rpm, (d) 800 Rpm and (e) 1000 Rpm and Optical profilometry images showing three- dimensional (3D) surface morphologies of (a') 200 Rpm, (b') 400 Rpm, (c') 600 Rpm, (d') 800 Rpm and (e') 1000 Rpm

Table 3. Estimation of COF

RPM	Load(N)	Radius of asperity	Pressure calculated	Calculated force (N)	Calculated COF
200	20	0.178	0.148	186.48	0.23
	40	0.164	0.254	319.16	0.27
	60	0.154	0.336	421.66	0.3
	80	0.152	0.436	547.71	0.31
400	20	0.217	0.222	278.61	0.15
	40	0.201	0.382	479.20	0.18
	60	0.184	0.479	601.16	0.21
	80	0.154	0.447	561.48	0.3
600	20	0.163	0.125	156.57	0.27
	40	0.154	0.224	281.47	0.3
	60	0.142	0.285	358.54	0.36
	80	0.132	0.330	415.02	0.41
800	20	0.176	0.147	184.13	0.23
	40	0.163	0.249	312.58	0.27
	60	0.150	0.316	396.86	0.32
	80	0.140	0.367	460.72	0.37
1000	20	0.154	0.112	140.86	0.3
	40	0.142	0.190	239.03	0.36
	60	0.140	0.275	345.54	0.37
	80	0.132	0.329	413.14	0.41

Fig 12 represents the comparison between values of COF through the nominal and derived through the proposed equation for varying rpm. The relationship between COF and load is proportional and shows similar increasing trends in each rpm. The difference between the values of the COF in actual and calculated is mainly due to the varying area of contact, as discussed earlier. Also, due to wear, the area of contact changes; hence, the COF range seems to deviate. At higher rpm the calculated area appears to be increased as the pressure considered is high for the nominal method during the particular rpm is high. In the proposed way, not much difference in values of COF is seen even for high rpm. The range of COF for the nominal method is between 0.2-0.6, and the range obtained from the derived equation is from 0.2 – 0.4. As the surface area during the initial stage of braking is the same, the initial values of COF for all the rpm are similar in the range between 0.2-0.25. This changes gradually with a change in the contact pressure and wears off the interfacing materials due to friction. In fig 12 (a), the value of COF after 40N can be seen increasing drastically for the nominal calculation method. Whereas, for the derived form, the value of COF increases moderately as only the points of contact between the interface are considered. This is the main perk of contact mechanics, which aids in visualizing and evaluating the actual contact area in the tribological interface. For higher rpm, i.e., for 800 and 1000 rpm, the value of COF is seen to rise linearly due to less contact time and increased pressure.

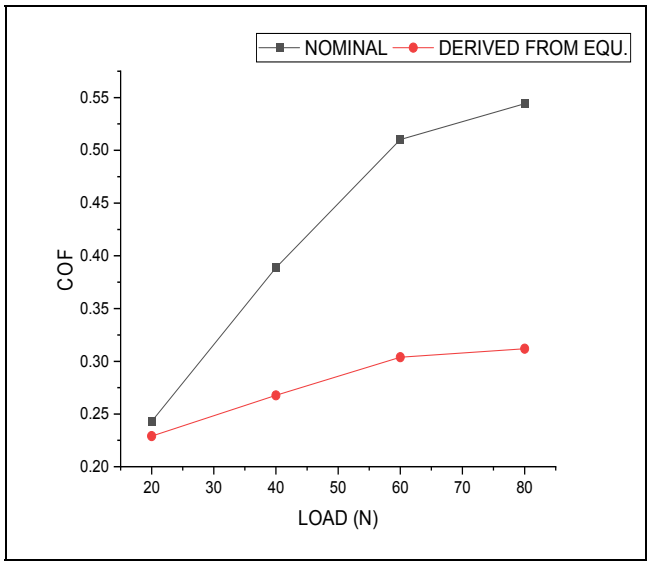

(a) 200 RPM

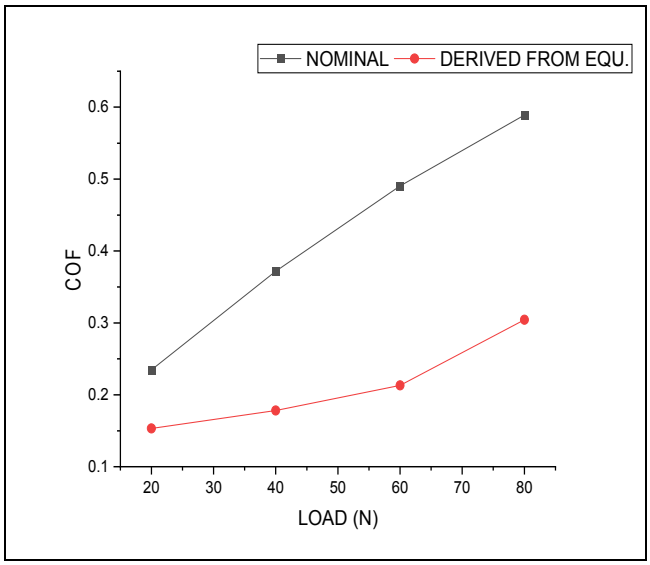

(b) 400 RPM

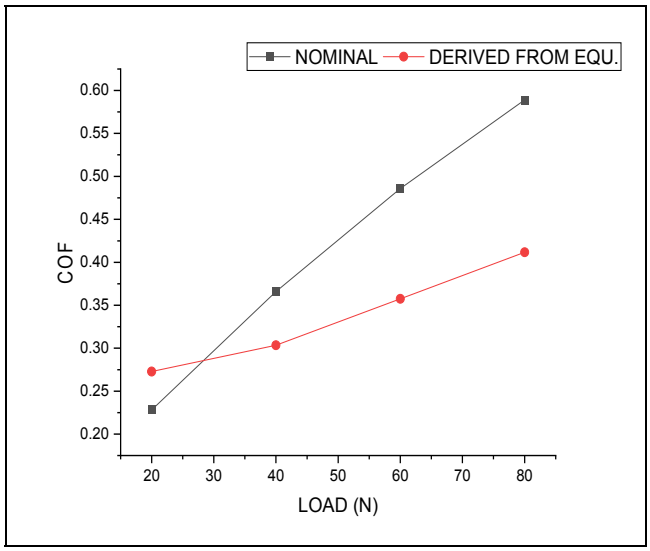

(c) 600 RPM

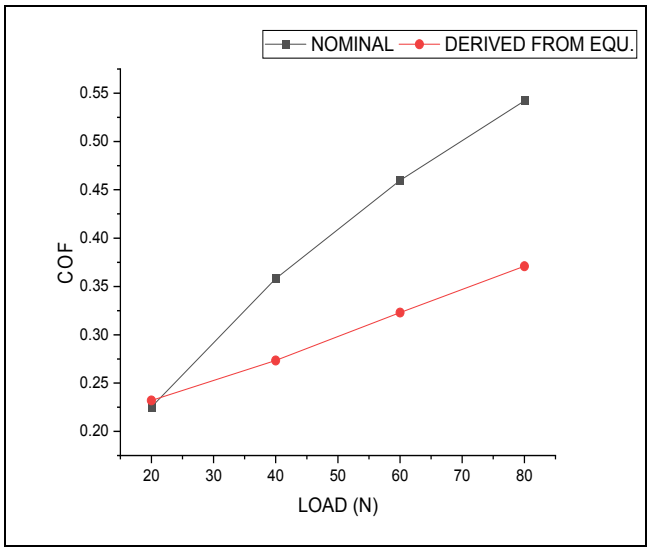

(d) 800 RPM

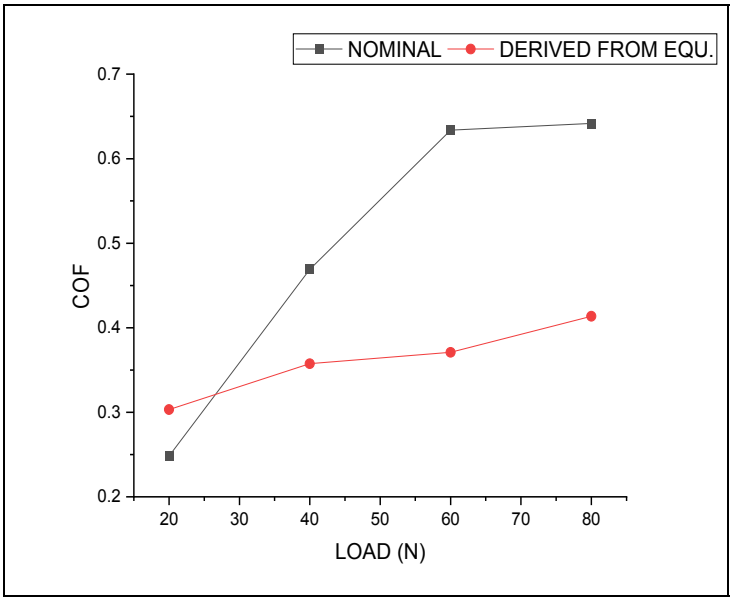

(e)1000 RPM

Figure 12. Comparison of COF through the nominal and derived method

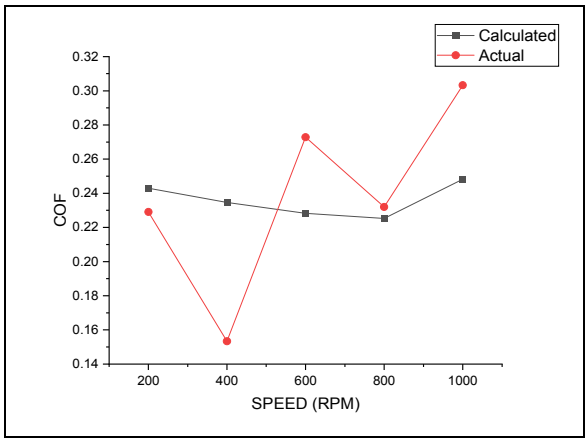

(a) Constant load 20N

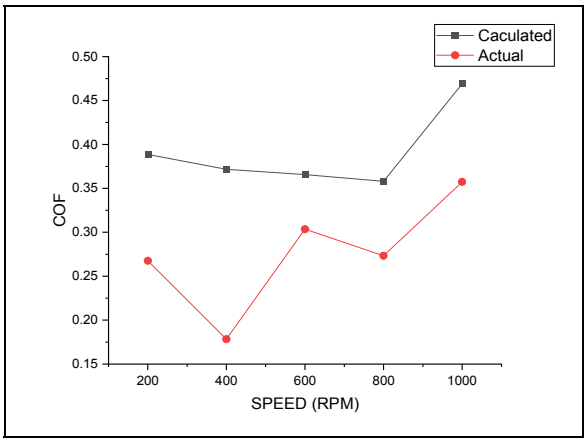

(b) Constant load 40N

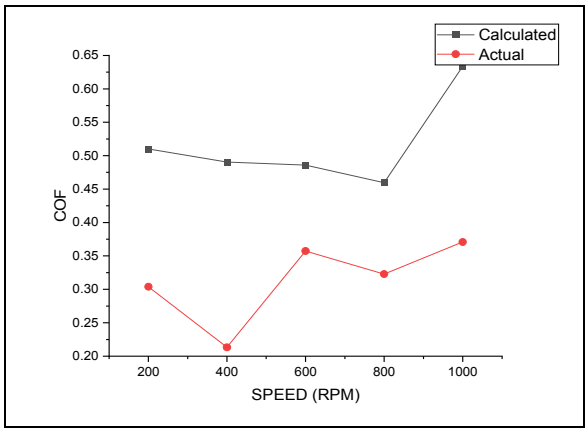

(c) Constant Load 60 N

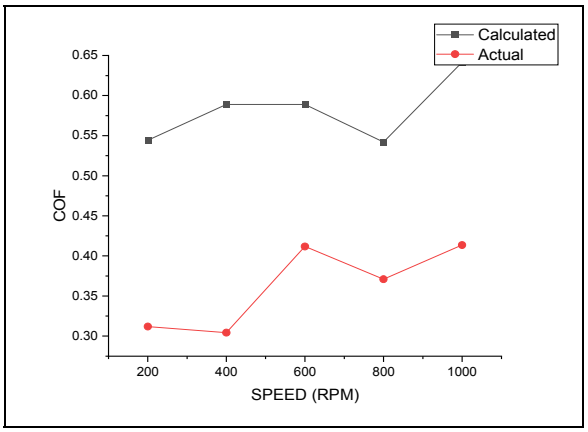

(d) Constant load 80 N

Figure 13.Comparison of COF for various RPM at constant load

On the macro and micro scale, the tribological cha–racteristics of brake pad/disc depend on the formation, growth, and disintegration of contact plateaus, shape adaptation, and thermal-induced deformation [4]. In fig. 13 (a-d) represents the comparison of COF for various RPM at constant load. As it can be seen, there is fluctuation in values of COF at different rpms; this is mainly due to wear and wear debris getting trapped into the brake pad and disc interface. The wear debris increases the area of contact, forming a third body layer between the interface of the brake pad and disc; as a consequence, a sudden spike of COF value at 600 rpm can be seen for the loads. And the decrease in the value can be seen at 800 rpm due to wear.

Fig 14 (a-d) shows the interface pressure for varying loads at particular rpm. The pressure value through the nominal method disports a linear trend from 200rpm to 800 rpm. The pressure values calculated through the proposed method have been elevated for each applied load. The interface pressure is inversely proportional to the area of contact. The increased pressure values depict the smaller contact area, i.e., the contacting interface is between the heightened asperities and the brake disc surface. Maximum value of interface pressure is 0.4 N/mm^2, which can be acceptable for a dynamic system operating in high speed and relatively closed environ–ment. Decreasing trend of CoF at large velocities can be described as due to the high-velocity time required for asperity to contact also less. Thus, deformation reduces, which further reduces the real area of contact. Hence, CoF is lowered due to increasing velocity [26].

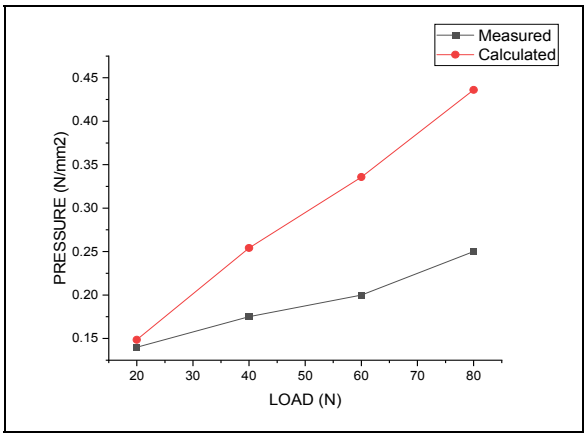

(a) 200 RPM

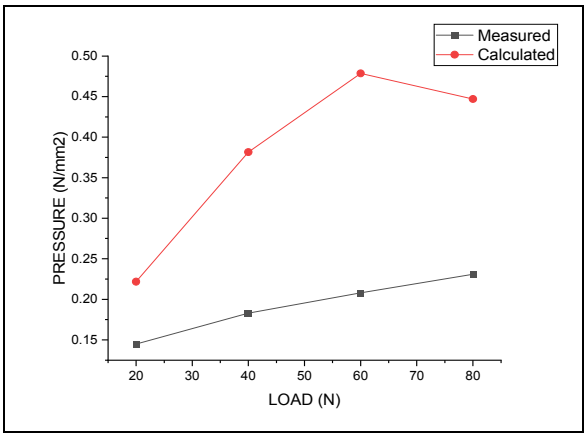

(b) 400 RPM

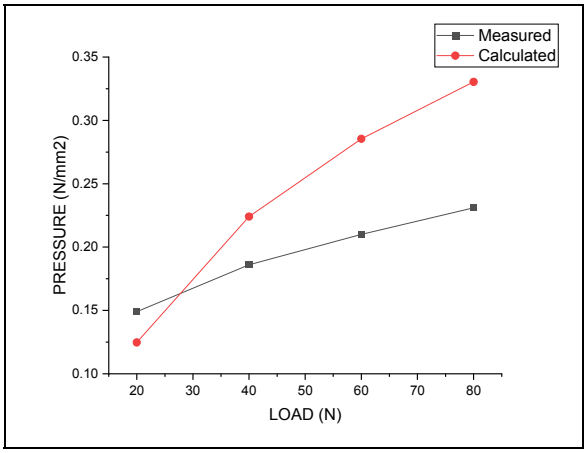

(c) 600 RPM

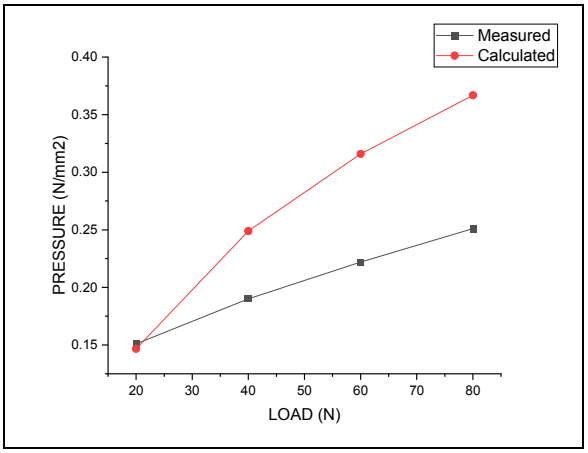

(d) 800 RPM

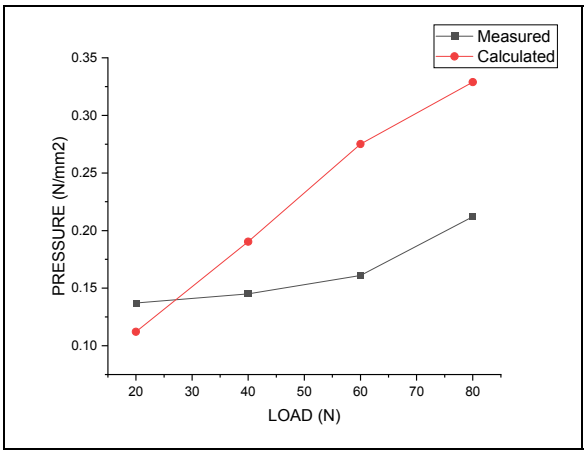

(e) 1000 RPM

Figure 14. Comparison of interface pressure for various loads at constant rpm.

6. CONCLUSIONS

A mathematical model is proposed in the present work for calculating the actual coefficient of friction, which is derived by using basic concepts of contact mechanics and material properties. The analytical evaluation shows the mathematical model's application to a passenger vehicle's brake system. Also, the MATLAB program is designed for simulating actual interface conditions between the brake pad and disk. In addition, experimental evaluation was carried out on the different sets of brake pads of passenger vehicles under various speed, pressure, and loading conditions on the novel brake test rig. Samples of the brake pad were prepared after, and further analysis was carried out for surface topography to understand interface conditions during the braking operation. Finally, the experimental and analytical results were compared for validation:

- The analytical evaluation and experimental evaluation show a similar trend for COF. The value of COF obtained through the proposed method is between the range of 0.3-0.5, which is the same for both evaluations and falls in the normal range as per reported literature. It has been seen that, as speed for the system increases, the COF is slightly elevated at the same loading condition; this is due to an increase in the contact form of secondary plateaus in the brake pad interface, as shown in fig. 12 (a-d).
- Pressure distribution on the brake pad surface depends upon the actual asperity's radius of contact. Increase in nominal pressure causes deformation in asperities, thus affecting the pressure distribution. The highest value of interface pressure was 0.47 N/mm^2, showed at 400rpm for 60N load.
- Surface properties like surface roughness and rigidity modulus affect a material's friction behavior. Thus, considering them helps estimate and predict friction forces affecting the system more accurately.
- The developed novel brake test rig can be effectively used to assess the frictional behavior of different brake pads for various operating conditions. This test rig also reduces the time required for calculating the coefficient of friction.
- The analytical values are consistent with experimental observations and can be used to estimate the friction coefficient for developing an efficient brake system using different brake pad materials, considering the surface values of the friction material and operating conditions of the brake system.

ACKNOWLEDGMENT

The authors would like to thank Technical Education Quality Improvement Program (TEQIP-III), VJTI, for providing the financial support.

REFERENCES

[1] Amrish, P.: Computer-aided design and analysis of disc brake rotors, Advances in Mechanical Engineering, Vol. 5 (2), pp. 1-13, 2016.

[2] Khairnar, H. P., Phalle, V. M. Mantha, S. S.: Estimation of automotive brake drum−shoe inter–face friction coefficient under varying conditions of longitudinal forces using Simulink, Friction3(3): 214–227, 2015.

[3] Ostermeyer, G.P. and Muller, M.:New insights into the tribology of brake systems, Automobile Engi–neering, Vol. 222, pp. 1167-1200, 2007.

[4] Barecki, Z., Scieszka, S.F.:A mathematical model of brake shoe and the brake path system, N&O Journal: 13–17 ,1987.

[5] Fernandez J G.:*A Vehicle Dynamics Modelfor riving Simulators*, Master's thesis,Chalmer University, Sweden, 2012.

[6] Kapoor, A., Tung, S. C., Schwartz, S. E., Priest, M., Dwyer-Joyce, R. S.: *Automotive Tribology*. CRC Press LLC, 2001.

[7] Fowler A C.: *Techniques of Applied Mathematics*. Mathematical Institute, Oxford University, 2005.

[8] Dubar, A. L. et al.: A methodology for the modelling of the variability of brake lining surfaces. Wear, 289:145–159, 2012.

[9] Eriksson,M., Bergman,F., Jacobson,S.: On the nature of tribological contact in automotive brakes, Wear, Vol. 252, pp. 26–36, 2002.

[10] Ostermeyer, G.P.: On the dynamics of friction coefficient, Wear, Vol. 254, 852–858,2003.

[11] Verma, P. C., Menapace,L., Bonfanti,A.,Ciudin, R., Gialanella,S. and Straffelini, G.: Braking Pad-Disc System: Wear Mechanisms and Formation of Wear Fragments, Wear, Vol. 322-323, pp. 251–258,2015.

[12] Degenstein,H.: Dynamic Measurement of the Forces in the Friction Area of a Disc Brake during a Braking Process, in FISITA 2006, World

[13] Automotive Congress, Yokohama, Japan, 2006.

[14] Blanco-Lorenzo, J., Santamaria, J., Vadillo, E. G., Correa,N.: A contact mechanics study of 3D fricti–onal conformal contact, Tribology International 119 (2018) 143–156,2018.

[15] Eriksson, M., Jacobson, S.: Tribological surfaces of organic brake pads, Tribology International, 33 (12):817–827, 2000.

[16] Österle, W., Dörfel, I., Prietzel, C., Rooch, H., Cristol-Bulthé, A.-L., Degallaix, G., Desplanques, Y.: A comprehensive microscopic study of third body formation at the interface between a brake pad and brake disc during the final stage of a pin-on-disc test. Wear, 267(5-8):781–788, 2009.

[17] Ali, B.and Mostefa, B.: Thermomechanical Model–ling of Disc Brake Contact Phenomena, FME Transactions, VOL. 41, No 1, pp. 59-63, 2013

[18] Ćirović, V. and Aleksendrić, D.: Development of neural network model of disc brake operation,FME Transactions, Vol. 38, No. 1, pp. 29-38, 2010.

[19] Bhushan, B.: Contact mechanics of rough surfaces intribology: Multiple asperity contact. Tribology Letters, 4(1):1–35, 1998.

[20] Nosonovsky, M. and Bhushan, B.: Multiscale friction mechanisms and hierarchical surfaces in nano- and bio-tribology. Materials Science and Engineering: R: Reports, 58(3-5):162 – 193, 2007.

[21] Dankowicz, H.: On the modeling of dynamic friction phenomena. ZAMM Zeitschrift fur Angewandte Mathematik und Mechanik, 79(6):399–409, 1999.

[22] Oden, J.T., Martins, J.A.C.: Models and computa–tional methods for dynamic friction phenomena. Computer Methods in Applied Mechanics and Engineering, 52(1-3):527–634, 1985.

[23] Ćirović, V., Aleksendrić, D.: Dynamic Modelling of Disc Brake Contact Phenomena, FME Tran–sactions, Vol.39, No.4, 2011.

[24] Feldmanis, J.: Mathematical modelling of disc brake friction lining heat and wear, Engineering for rural development Jelgava, 29.-30.05,2008.

[25] Day, A. J.: *Braking of RoadVehicles*, Elsvier,2014.

[26] Giri, N.K.:*Automotive Mechanics,* New Delhi (India): Khanna Publisher, 1990

[27] Österle, W. and Dmitriev, A.I..: Functionality of conventional brake friction materials - perceptions from findings observed at different length scales. Wear, 271(9-10):2198–2207, 2011.

[28] Ali, B., Bakar,A. R. A.and Mostefa,B.: Thermal and structural analysis of disc brake assembly during single stop braking event, Australian Journal of Mechanical Engineering, 2015.

[29] Greenwood, J. A.,Williamson, J. B. P..: Contact of Nominally Flat Surfaces**,** Proceedings of the Royal Society of London. Series A, Mathematical and Physical Sciences, Vol.295, No. 1442., pp. 300-319,1996.

[30] Popov, V. L.: *Contact Mechanics and Friction*, Springer, 2010.

[31] Hohmann, C., Schiffner, K., Oerter, K. and Reese, H.: Contact analysis for drum and disk brakes using ADINA, Computers and Structures, Vol. 72, pp. 185-198,1999.

[32] Aleksendrić, D. and Duboka, Č.: A Neural Model of Automotive Cold Brake Performance, FME Transactions, VOL. 35, pp. 9-14, 2007.

[33] Oday I. Abdullah, Josef Schlattmann and Michael Lytkin: Effect of Surface Roughness on the Ther–moelastic Behaviour of Friction Clutches, FME Transactions, VOL. 43, No 3, pp. 241-248, 2015.

NOMENCLATURE

M	Mass of the vehicle (kg)
F_D	Force applied by the driver
N_1	Dynamic normal reaction at the road surface of the front axle under braking conditions (N)
N_2	Dynamic normal reaction at the road surface of the rear axle under

	braking conditions (N)
F_f	Brake force exerted by the brakes on the front axle under normal braking conditions on the road (N)
F_r	Brake force exerted by the brakes on the rear axle under normal braking conditions on road (N)
L_1	The horizontal distance from the front axle to the vehicle's center of gravity (m)
L_2	The horizontal distance from the rear axle to the vehicle's center of gravity (m)
h	Height of the center of gravity of the vehicle above the road surface (m)
E	Wheelbase (m)
W	Vehicle weight (N);
M_L	Mechanical leverage
H_L	Hydraulic leverage
W_T	Dynamic axle weight
D_w	Diameter of tire
D	Deceleration of the vehicle (m/s^2)
g	Acceleration due to gravity (¼ 9.81 m/s^2)
E	Young's Modulus
υ	Poisson's ratio
a	Contact radius

ИСПИТИВАЊЕ КОЕФИЦИЈЕНТА ТРЕЊА НА ИНТЕРФЕЈСУ КОЧИОНИХ ПЛОЧИЦА

АУТОМОБИЛА КОРИШЋЕЊЕМ ГРИНВУД-ВИЛИјАМСОН КОНТАКТ МОДЕЛА И НОВЕ ОПРЕМЕ ЗА ТЕСТИРАЊЕ

М. П. Ксхирсагар, Х. Кхаирнар

Производе се различити материјали кочионих плочица, сваки са својим јединственим саставом у недавној прошлости, а истовремено обављају исти задатак и тврде да су бољи од других. Чланак даје референце за различите аутомобилске кочионе плочице подвргнуте различитим радним условима. Ово истраживање развија аналитички приступ за процену ЦОФ-а и контактног радијуса за различите плочице диск кочнице, који се могу користити за пројектовање ефикасног аутомобилског кочионог диск-система под датим оптерећењем и брзином ротације. Коефицијент трења на интерфејсу јастучић-диск је истражен с обзиром на Гринвуд Вилијамсон (ГВ) модел и развијену нову опрему за испитивање трења. МАТЛАБ програм заједно са ФФТ је развијен да симулира топографију површине контактног интерфејса током процеса кочења, помажући у процени радијуса контакта. Топографија површине тестираних кочионих плочица је анализирана помоћу микроскопа са бесконачним фокусом да би се проверио радијус контакта. Коначно, референца је верификована експерименталним истраживањем користећи развијену опрему за испитивање и узимајући у обзир радне параметре.